GA–A23154

TRANSITIONS TO OVERSIZED CORRUGATED WAVEGUIDE

by
J.L. DOANE

JUNE 1999

GA–A23154

TRANSITIONS TO OVERSIZED CORRUGATED WAVEGUIDE

by
J.L. DOANE

This is a preprint of a paper to be presented at the Twenty-fourth International Conference on Infrared and Millimeter Waves, September 5–10, 1999, Monterey, California, and to be published in *The Proceedings.*

GA PROJECT 04945
JUNE 1999

Transitions to Oversized Corrugated Waveguide

J.L. Doane

General Atomics, P.O. Box 85608, San Diego CA 92186

Abstract

Data are presented for transitions from small rectangular waveguide designed for: 99.9% mode purity to measure high power 31.75 mm components at 94 GHz; and 90% efficiency for 63.5 mm waveguide measurements from 50-100 GHz and 100-180 GHz.

Introduction

Oversized corrugated waveguide propagating the HE_{11} mode is very useful for low-loss transmission. Transitions to this waveguide from small rectangular waveguide are required for two main purposes: 1) for low power testing of high power transmission line components, usually narrow band; and 2) for launching and receiving signals for long distance transmission, usually broadband.

Quasi-optical transitions with mirrors have had 97% or more mode purity over a narrow band. Transitions using a lens have typically 20% absorption loss in the lens plus reflection loss. The small rectangular-to-circular waveguide transition at the input to the scalar feed horn in these transitions is typically narrow band.

We have developed two other types of transitions for these applications: 1) a "mode converter type" and 2) a "horn reflector type". The mode converter type produces a very high purity (~99.9%) HE_{11} mode in a narrow band and is best suited for corrugated waveguides with diameter-to-wavelength ratios up to about 15. The horn reflector type operates over bandwidths up to 2:1 with an efficiency of about 90% and works best for diameter-to-wavelength ratios exceeding 10.

"Mode Converter" Transitions

These transitions have four sections: 1) a standard rectangular-to-small circular waveguide transition at the input, 2) a diameter taper propagating TE_{11} in smooth waveguide, 3) a converter to HE_{11} with a constant internal diameter and corrugation depth decreasing from ~$\lambda/2$ to $\lambda/4$, and 4) a diameter taper with constant corrugation depth. When used below cutoff of higher modes, the first section has no unwanted mode conversion.

To optimize the other three sections, we developed computer codes using numerical integration of the coupled mode equations. The coupling coefficients for diameter tapers are well known [1]. The propagation constants in the corrugated waveguide sections were calculated using space harmonic analysis [2]. A scattering matrix formalism [3] was used to calculate the mode scattering at the junction from smooth waveguide to waveguide with a nominal corrugation depth of $\lambda/2$.

The codes for the diameter tapers include modes that are cutoff on the small end by setting the coupling to zero except when the mode is above cutoff. The coupling coefficients have a weak singularity at cutoff. Nevertheless, numerical studies indicated that the calculated mode conversion to such modes is not sensitive to the exact location above cutoff where coupling to these modes is first considered in the numerical integrations. Diameter variations with no discontinuities were also chosen to avoid sensitivity to small errors.

The coupling coefficients for the TE_{11}-to-HE_{11} converter are proportional to the derivatives with respect to corrugation depth of the propagation constants of the coupled modes [4]. Since the propagation constants decrease with decreasing depth and vary rapidly near cutoff, the output diameter of the smooth diameter taper should not allow modes to propagate that are just slightly above cutoff.

Transitions to 31.75 mm corrugated waveguide were made for use near 60, 94, and 110 GHz. Figure 1 shows an electroformed transition for 94 GHz with a total length of 280 mm (11 in.).

The mode purity was estimated by measuring the transmission through two identical transitions, as in Fig. 2. Since all unwanted modes are cutoff at the small ends of the transitions, any mode conversion will cause resonances from these trapped modes. The level of an unwanted mode can be determined from the depth of the resonances and the attenuation of that mode between the cutoff points [5]. Since this attenuation is typically small, one of the measurements in Fig. 2 used a styrofoam section inserted near the junction of the two transitions to increase the attenuation by about 0.3 dB. The maximum measured resonance depths were 1 dB and 0.4 dB without and with the

Figure 1. Electroformed transition from WR10-to-31.75 mm corrugated waveguide for 92–96 GHz.

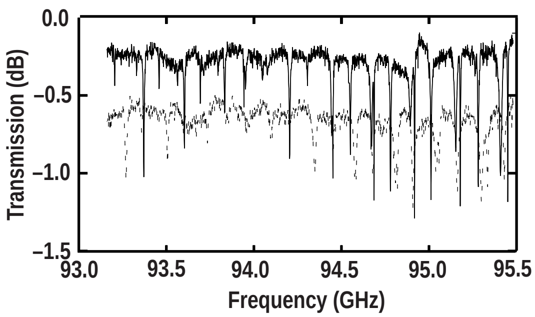

Fig. 2. Transmission through two transitions of Fig. 1, with and without a 25 mm long section of 31 mm diameter styrofoam inserted near the junction of the transitions.

styrofoam, respectively. Assuming the spurious mode attenuation is 0.3 dB and 0.6 dB for these two cases, the theory of Ref. 5 indicates a maximum spurious mode level 28 dB below the HE_{11} mode.

"Horn Reflector" Transitions

These transitions are made with three sections:1) a rectangular-to-square waveguide taper, 2) a truncated section of conical corrugated horn, and 3) a miter bend housing with a paraboloidal mirror and a corrugated waveguide inserted in the output bore. The taper is attached to the horn, which in turn slides into the input bore of the housing. There is no input transition from rectangular to circular waveguide which may cause mode conversion at higher frequencies.

By tapering the horn at a reasonably small angle, the spurious mode power generated at the curved mirror is kept small. To estimate this power, we use the analysis of Murphy [6], which applies to the distortion of a Gaussian beam, which is very similar to the HE_{11} mode. With a horn taper angle of 12°, the spurious mode power excited by amplitude and phase mismatch at the mirror is less than 1%, and loss to cross-polarized power is less than 2%. An estimated 0.5% additional loss is caused by power from the horn that spills over the ends of the mirror.

The rectangular taper shape is designed to match the HE_{11} mode in the truncated corrugated horn. A field in square waveguide that is tapered in both planes couples well to the HE_{11} mode in corrugated waveguide [7]. The H-plane dimension is flared rapidly to the 12° angle while maintaining the field taper in the H-plane. The E-plane dimension is slowly tapered at the beginning of the taper and then is flared rapidly to 12° to generate the hybrid TE_{12}/TM_{12} mode with the proper amplitude and phase to generate a field taper in the E-plane.

To design the E-plane taper, it was convenient to use paraxial approximations to the equations for the total field [8], similar to the approximation that yields the equations for Gaussian beams. We write the total electric field as $E_y = cos(\pi x/a)\, v(y,z)\, exp(-jkz)$ and assume that $v(y,z)$ is slowly varying with z. The wave equation then becomes the parabolic equation $2jk(\partial v/\partial z) = -(\pi/a)^2\ v + \partial^2 v/\partial y^2$. The boundary condition at $y = \pm b/2$ is $\partial v/\partial y = -j0.5\ kvb'(z)$.

Figure 3 shows a transition from 2 mm × 1 mm waveguide to 63.5 mm corrugated waveguide, designed for 100 to 180 GHz. The calculated efficiency from the rectangular waveguide input to the HE_{11} mode in the truncated horn was 93% or greater over this bandwidth, not including ohmic losses. Including the 3.5% losses at the mirror, we get an estimated efficiency of 89.5% or more. The measured insertion loss through two back-to-back transitions averaged about 11% per transition near 110 GHz and 15% per transition near 165 GHz. The radiation patterns measured near 110 and 165 GHz matched quite well the radiation patterns of an ideal HE_{11} mode. Transitions from WR15 to 63.5 mm waveguide gave similar results in the 50 to 100 GHz band.

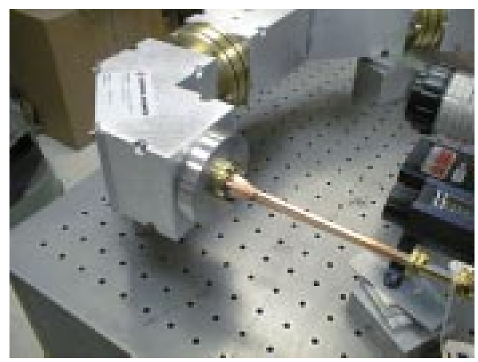

Fig. 3. Transition from WR8 to 63.5 mm corrugated waveguide for 100–180 GHz.

References

[1] J.L. Doane in K J. Button, Infrared and Millimeter Waves, Vol. 13, Chapter 5, Academic Press (1985).

[2] P.J.B. Clarricoats and A.D. Olver, Corrugated Horns for Microwave Antennas, Appendix, Peter Peregrinus Ltd. (1984).

[3] G.L. James, IEEE Trans. Microwave Theory Techniques, MTT-29, 1059 (1981).

[4] J.L. Doane, Int. J. Infrared and Millimeter Waves **14**, 363 (1993) Eq. (12).

[5] A.P. King and E.A. Marcatili, Bell System Technical Journal **35**, 899 (1956) Fig. 3.

[6] J.A. Murphy, Int. J. Infrared and Millimeter Waves **8**, 1165 (1987).

[7] C.P. Moeller and J.L. Doane, Proc. of the 15th Int. Conf. on Infrared Millimeter Waves, Orlando (1990).

[8] M.A. Shapiro and S.N. Vlasov, Proc. URSI Int. Conf. on Electromagnetic Theory, Stockholm, 240 (1989).